Journal of Hazardous Materials, 16 (1987) 215–230
Elsevier Science Publishers B.V., Amsterdam — Printed in The Netherlands

3-D NUMERICAL SIMULATION OF HEAVY GAS DISPERSION

Ø. JACOBSEN

SINTEF, Div. of Fluid Dynamics, Section of Aero- and Gas Dynamics, 7034 Trondheim-NTH (Norway)

and B.F. MAGNUSSEN

Div. of Thermodynamics, Norwegian Institute of Technology, 7034 Trondheim-NTH (Norway)

(Received 20 October 1986; accepted 23 February 1987)

Summary

A three-dimensional numerical program has been developed for simulation of heavy gas dispersion. The k–ϵ model with standard constants has been used for calculation of the diffusion coefficients where the effect of density gradients on the mixing process is accounted for by applying correction factors given as functions of the local Richardson number. The results of a numerical simulation of the Thorney Island Trial 008 are in good agreement with the experimental data.

1. Introduction

In developing a general numerical program for fluid dynamic computation one uses a numerical method that consists of a finite difference procedure for solving the momentum and continuity equations with additional equations relevant to the modelling techniques and the problem at hand. The present model is based on the Patankar and Spalding method [1] which uses the continuity equation as a pressure-correction with a subsequent continuity-satisfying velocity field and is similar to the model used by Deaves [2,3].

This procedure is basically designed for stationary problems but has also been applied to transient phenomena [4,5]. Here we have extended the method to a three dimensional transient flow situation. In particular, we have considered the spreading of a heavy gas in the atmosphere. Gravity related terms are included in the equations without the use of the Boussinesq approximation which has been applied by Riou et al. [6]. The diffusion coefficients are modified through empirical factors given as functions of the local Richardson number [7]. Constants used in these modifying functions are taken from a two-dimensional computation which has been verified through comparison with wind tunnel tests [5].

0304-3894/87/$03.50

2. The system of equations

2.1 The basic equations

The transient isothermal release of a gas into the atmosphere may be described by at least five differential equations. We need two mass conservation equations, one for the total mass and one for the mass of the released gas. Conservation of momentum requires three equations, one for each direction in space.

The flow is assumed to be turbulent and the variables represent time-mean values. Several terms in the equations above are time averaged quantities of the fluctuating part of the different variables and have to be expressed as functions of the relevant variables.

Depending upon the model chosen, we may have to introduce new variables which require additional equations to be solved, from the simple algebraic expressions to the more complex differential equations.

In our case we chose the equations using the k-ϵ model. Thus two additional differential equations are used, one for the conservation of turbulent kinetic energy and one for its rate of dissipation.

All these equations can be written in the following general form

$$\frac{\partial}{\partial t}(\rho\phi)+\frac{\partial}{\partial x_j}(\rho v_j\phi)=\frac{\partial}{\partial x_j}\left[\Gamma_\phi\frac{\partial_\phi}{\partial x_j}\right]+S_\phi$$

where ϕ represents the general variable, Γ_ϕ is the diffusion coefficient, and S_ϕ the source term.

The particular form of the diffusion coefficients and source terms are given in Table 1.

The pressure is reduced with respect to the atmospheric hydrostatic pressure giving the gravity term in the vertical momentum equation proportional to the density difference.

The production of turbulent kinetic energy P is expressed as

$$P=\Gamma\left[2\left[\left(\frac{\partial u}{\partial x}\right)^2+\left(\frac{\partial v}{\partial y}\right)^2+\left(\frac{\partial w}{\partial z}\right)^2\right]+\left(\frac{\partial u}{\partial y}+\frac{\partial v}{\partial x}\right)^2+\left(\frac{\partial u}{\partial z}+\frac{\partial w}{\partial x}\right)^2+\left(\frac{\partial v}{\partial z}+\frac{\partial w}{\partial x}\right)^2\right]$$

In addition to P, turbulent kinetic energy is produced or reduced due to density fluctuation with a term proportional to $\overline{g\rho' w'}$. When ρ is substituted with the concentration c through the relation given below and the term is modelled as a gradient diffusion term the buoyant production term can be given the form shown in the table below. Corresponding terms with respect to buoyant production have been neglected in the equation for the dissipation. The result of

TABLE 1

Diffusion coefficients and source terms

Equation	ϕ	S_ϕ	Γ_ϕ
Mass conservation	ρ	0	0
Concentration (mass fraction)	c	0	Γ/Pr_c
x-momentum	u	$-\frac{\partial p}{\partial x}$	Γ
y-momentum	v	$-\frac{\partial p}{\partial y}$	Γ
z-momentum	w	$-\frac{\partial p}{\partial z}-(\rho-\rho_a)g$	Γ
Turbulent kinetic energy	k	$P-\rho\epsilon+\Gamma_c g\frac{\rho}{\rho_g}\frac{\rho_g-\rho_a}{\rho_a}\frac{\partial c}{\partial z}$	Γ/Pr_k
Dissipation	ϵ	$C_1\rho\frac{\epsilon}{k}P-C_2\rho\frac{\epsilon^2}{k}$	Γ/Pr_ϵ

this approximation will probably give a small error which is partly corrected using diffusion coefficients as functions of the Richardson number.

The diffusion coefficient is assumed to be given by

$$\Gamma=C_D\,\rho\,k^2/\epsilon\,\frac{1}{1+\beta_1\mathrm{Ri}}$$

The influence of the density stratification upon the mixing process is represented by the last factor in the expression above and is similar to the one used in Ref. [7]. It is given as a function of the local Richardson number

$$Ri=-g\frac{(1/\rho)\ (\partial\rho/\partial z)}{(\partial u/\partial z)^2}$$

The Prandtl/Schmidt number Pr_ϕ is expressed as

$$Pr_\phi=\alpha_\phi\,\frac{1+\beta_1 Ri}{1+\beta_2 Ri}$$

The values of the constants appearing in the expressions are given in Table 2.

The constants are given standard values except for β_1 and β_2 which are found from a two-dimensional simulation of a stationary release of heavy gas where a fence was placed some distance downwind from the source [5]. The result

TABLE 2

Values of constants

C_D	C_1	C_2	β_1	β_2	α_c	α_k	α_ϵ
0.09	1.44	1.92	5	25	0.7	1.0	1.3

of this calculation was compared with experimental data from a corresponding wind tunnel test.

In addition to the differential equations we have the following relations between the cloud density ρ, mass fraction c and the volume concentration c_{vol}.

$$\rho = \rho_a \left[1 + c(R_g/R_a - 1)\right]^{-1}$$

$$c_{vol} = c\,\rho/\rho_g$$

where R_g and R_a are the specific gas constants for the released gas and air respectively.

2.2 Boundary conditions

The domain of calculation is given as a rectangular box (Fig. 1) with one axis along the horizontal mean wind direction (x-direction). Assuming a constant wind direction during the spreading, the flow will be symmetric to the plane ABFE, and we consider therefore only half of the space influenced by the released gas. Along this symmetry plane we use $v = 0$ and $\partial/\partial n = 0$.

On the opposite plane DCGH and the upper boundary EFGH we have the same requirements in addition to $w = 0$. On the upwind boundary ABHE we use an input horizontal velocity profile for u while $v = 0$ and $w = 0$.

On the downwind boundary we assume the horizontal gradients to be negligible.

On boundaries such as ABCD, the velocity is set equal to zero. For the other variables we use $\partial/\partial n = 0$ and $k = \tau/0.3$, where τ is the shear stress.

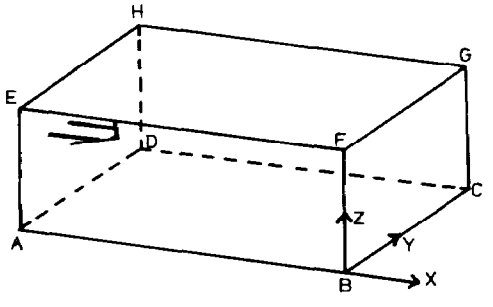

Fig. 1. Computational domain.

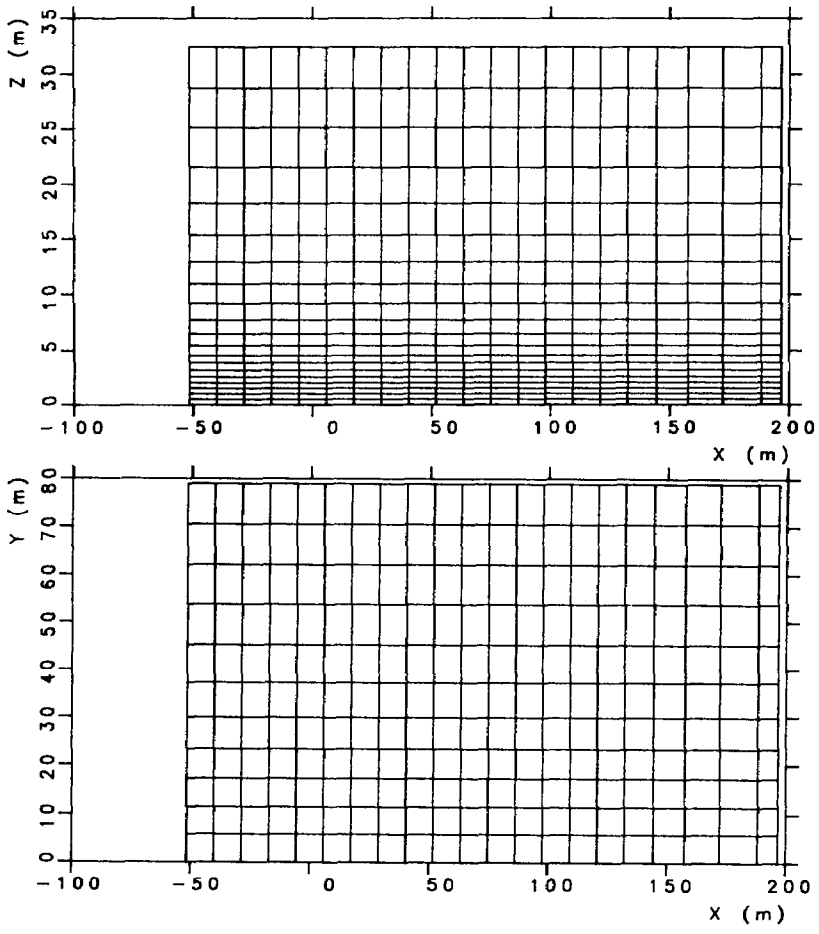

Fig. 2. Grid system in the vertical plane. Control volumes for scalar variables.

For points within the flowfield but in the immediate neighbourhood of solid boundaries the dissipation is given by $\epsilon = C_D^{3/4}\ k^{3/2}/d$, where d is the distance from the point to the boundary.

3. Numerical solution

The equations are discretized using the control volume method and a staggered grid for the velocity components are used.

The convective terms are evaluated using an upwind scheme, while the diffusion coefficients are interpolated assuming the inverse value to be linear between the grid points.

The continuity equation is transformed into a pressure correction equation

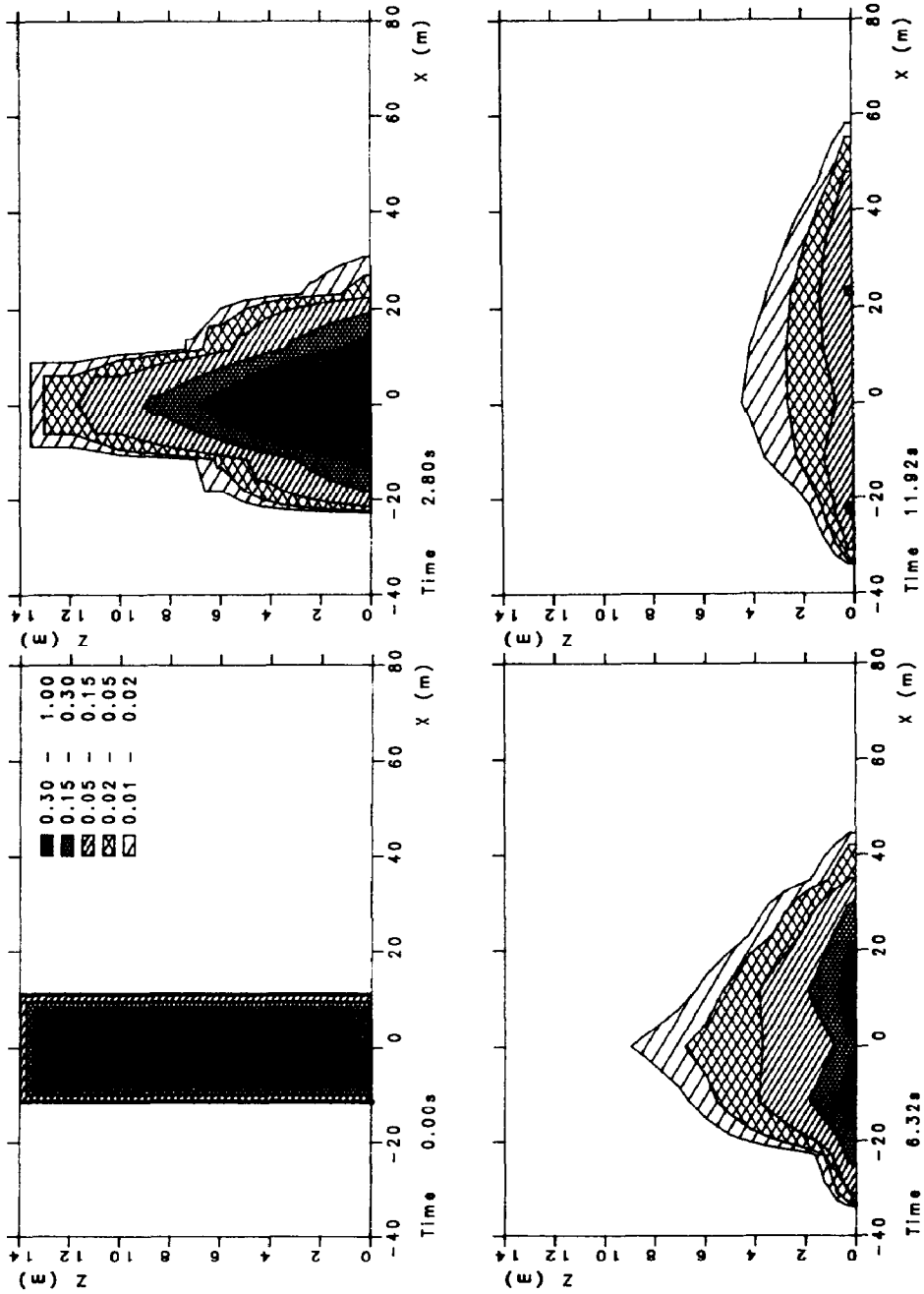

Fig. 3. Isoconcentration curves in the vertical plane for $y=0$ m.

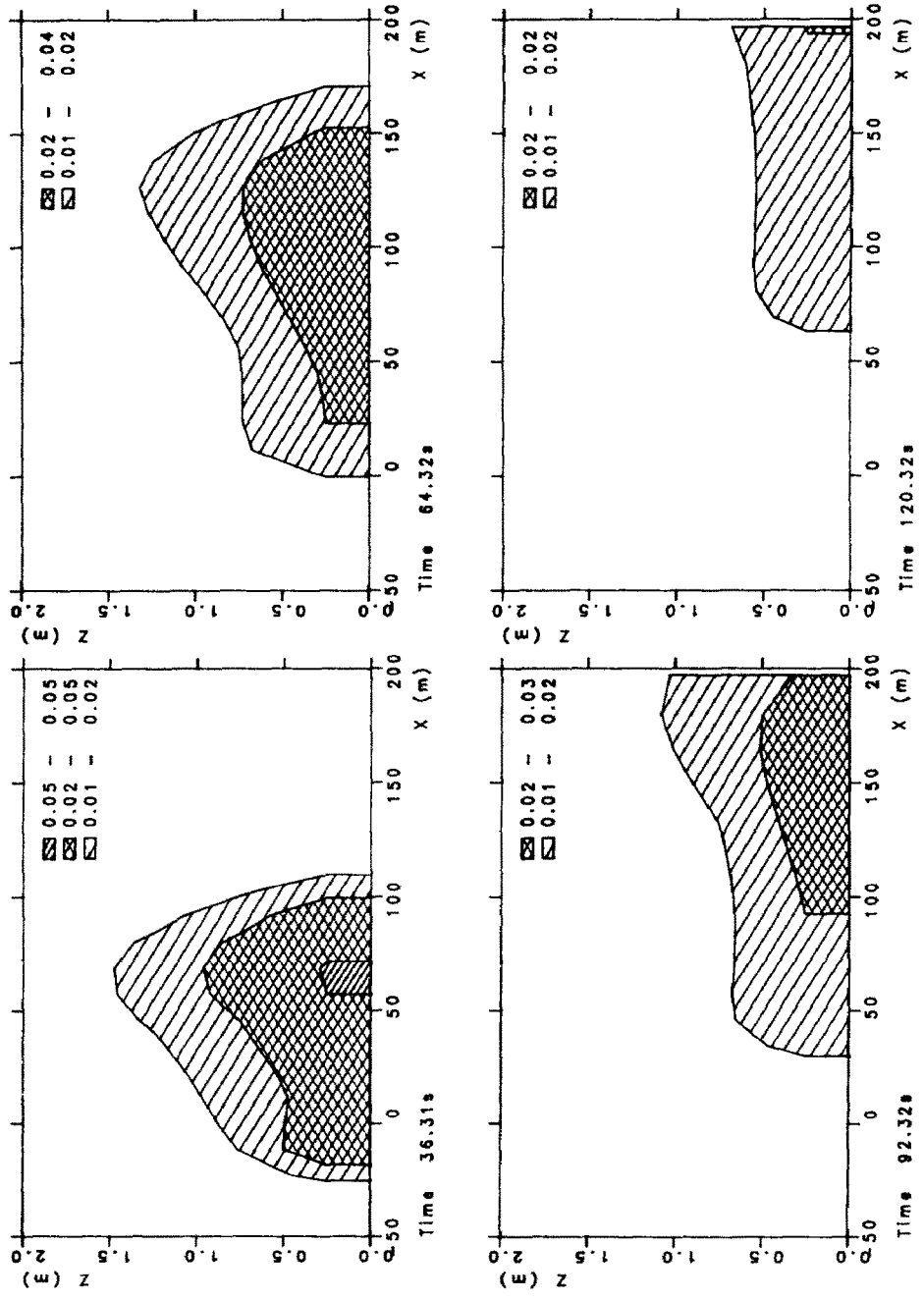

Fig. 4. Isoconcentration curves in the vertical plane for $y=0$ m.

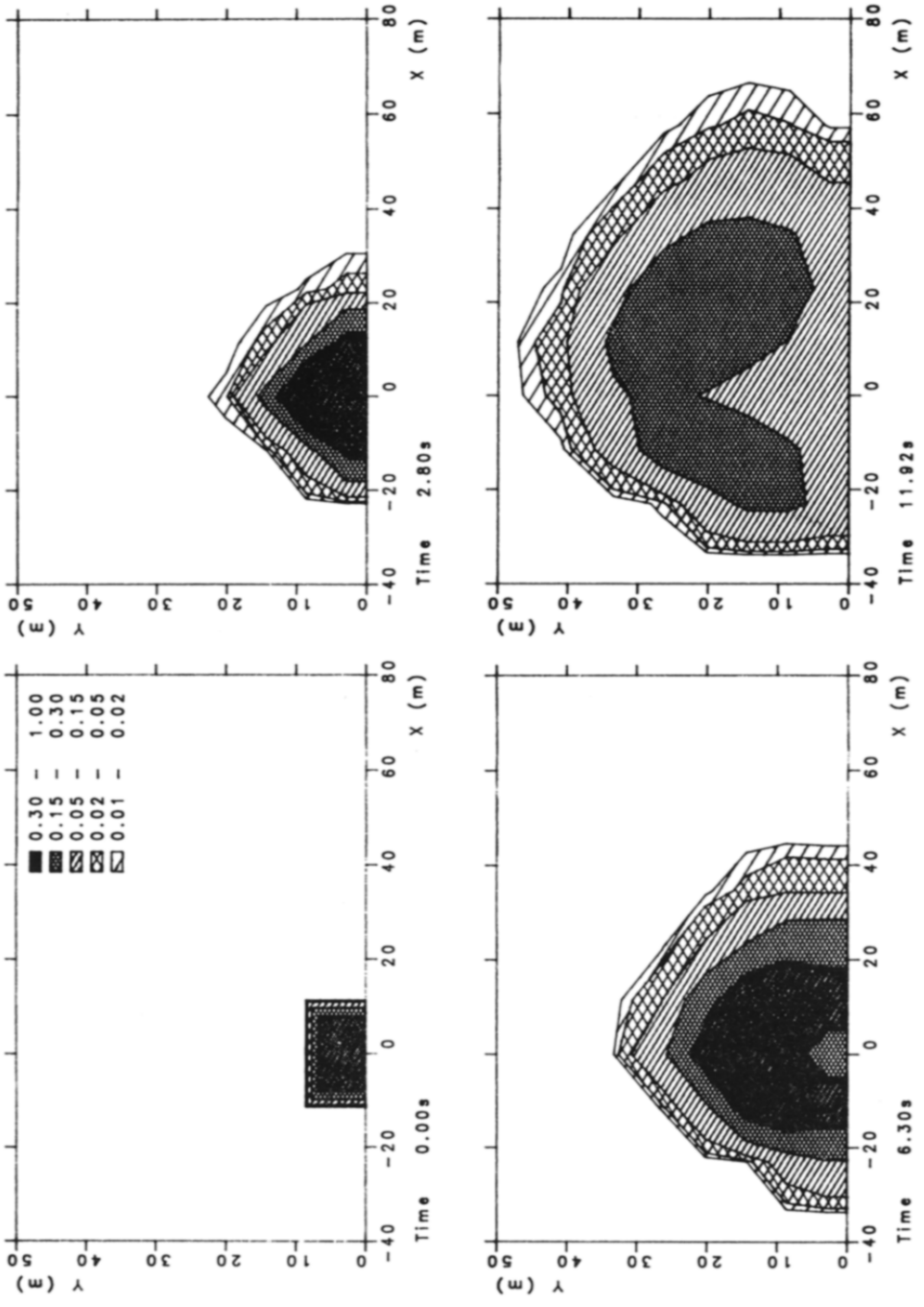

Fig. 5. Isoconcentration curves in the horizontal plane at the height of 0.4 m.

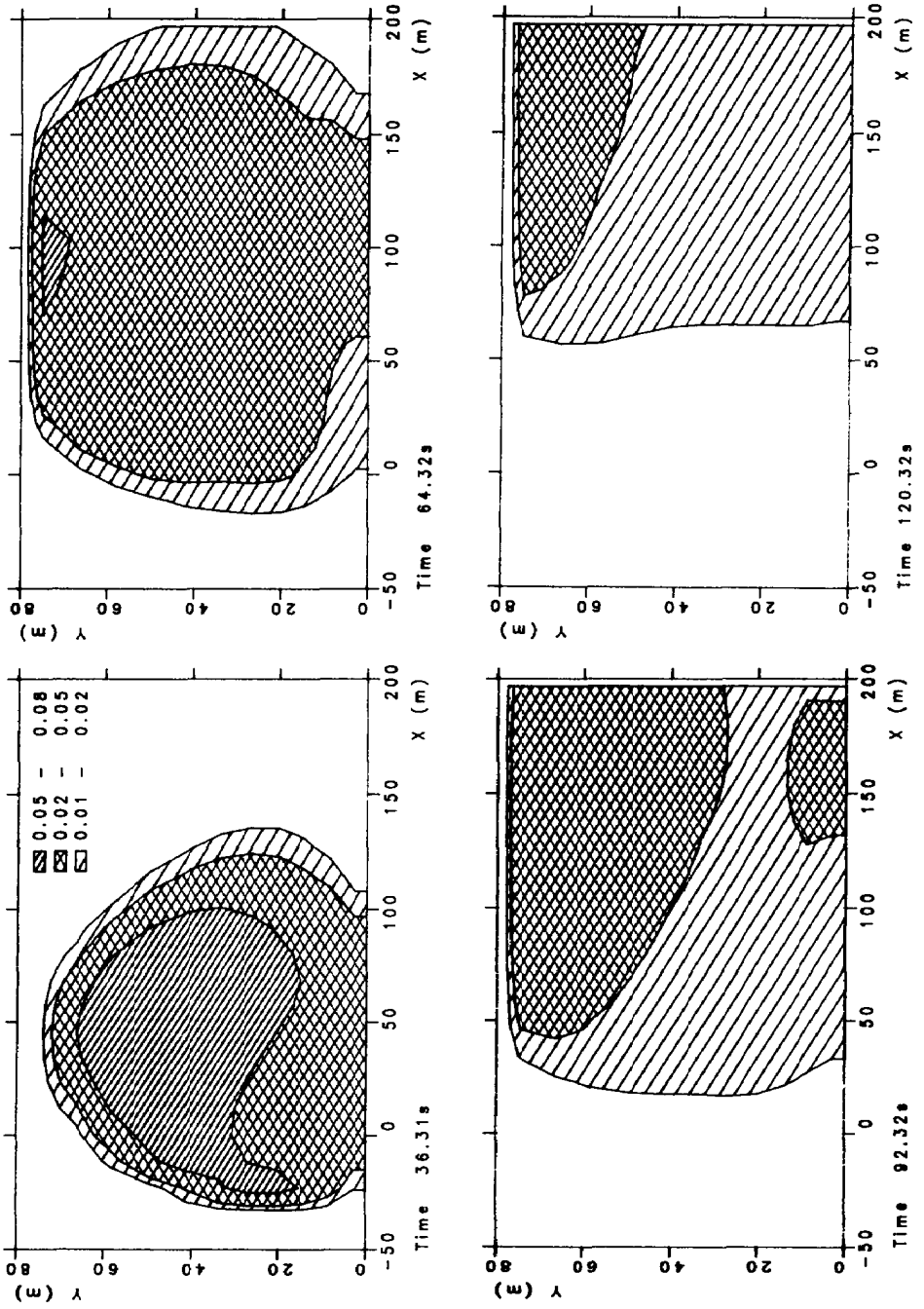

Fig. 6. Isoconcentration curves in the horizontal plane at the height of 0.4 m.

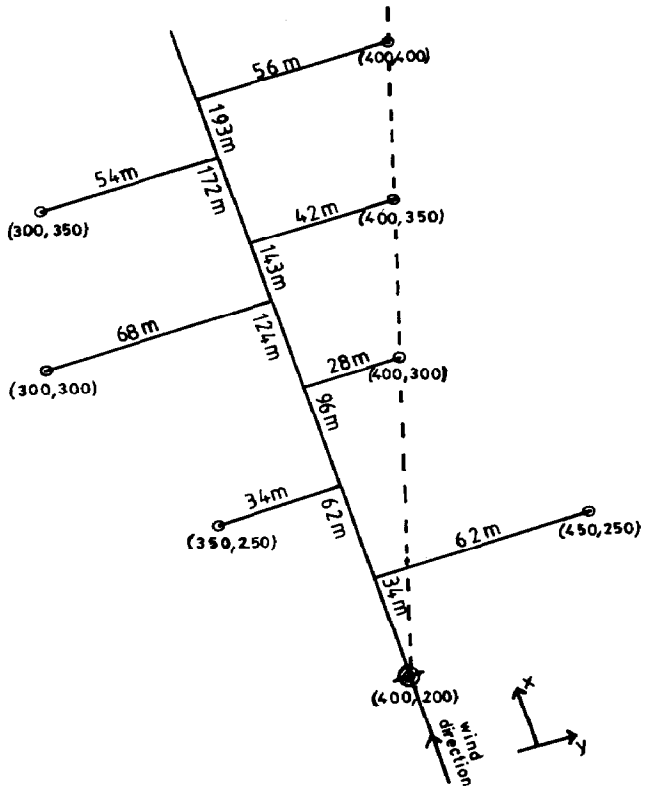

Fig. 7. Position of the measuring stations.

according to the numerical scheme given by Patankar and Spalding [1]. This tranformation is based upon a simple relation between the deviation in the velocity and pressure field.

3.1 The solution procedure

The method of solution is based upon the SIMPLE (Semi Implicit Method for Pressure Linked Equations) algorithm [1]. From an assumed pressure field the momentum equations are solved. Through the continuity equation the velocity and pressure are corrected until the equations are satisfied. Then the other equations are solved.

4. Simulation of the Thorney Island Trial 008

4.1 Input conditions and basic assumptions

The input velocity profile is assumed to be a logarithmic profile with a velocity of 2.40 m/s at the height of 10 m, and the roughness height is assumed to

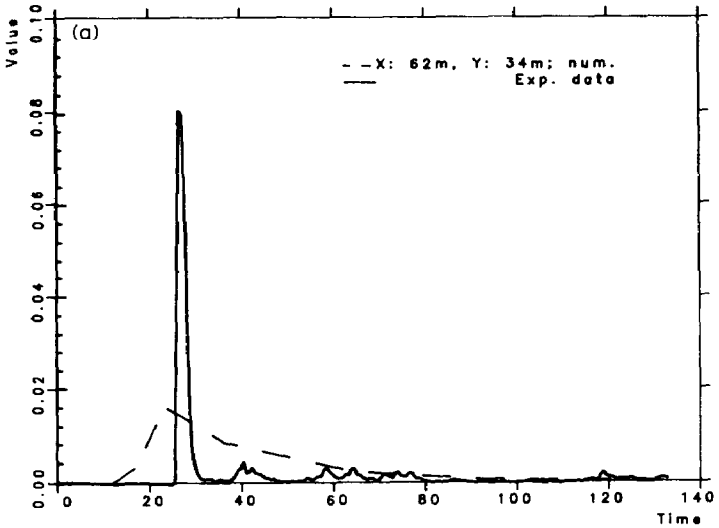

Fig. 8a. Concentration as function of time at the height of 2.4 m. Numerical simulation compared with experimental data. Location coordinates (350,250).

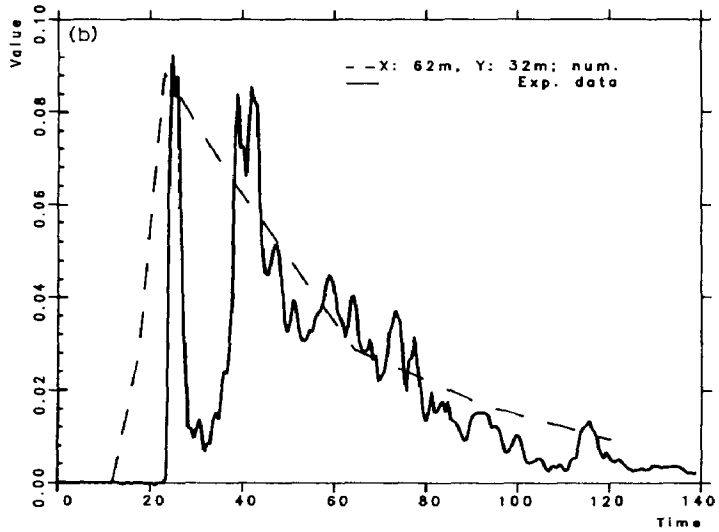

Fig. 8b. Concentration as function of time at the height of 0.4 m. Numerical simulation compared with experimental data. Location coordinates (350,250).

be 0.01 m. The domain of calculation spans the volume 260 m$\times$80 m$\times$33 m with the corresponding number of grid points equal to $23\times13\times22$. This is shown in Fig. 2. We consider in this case a release of heavy gas and the main part of the cloud will be near to the ground and the large density gradients found here. In this region we therefore use the smallest grid dimension in the

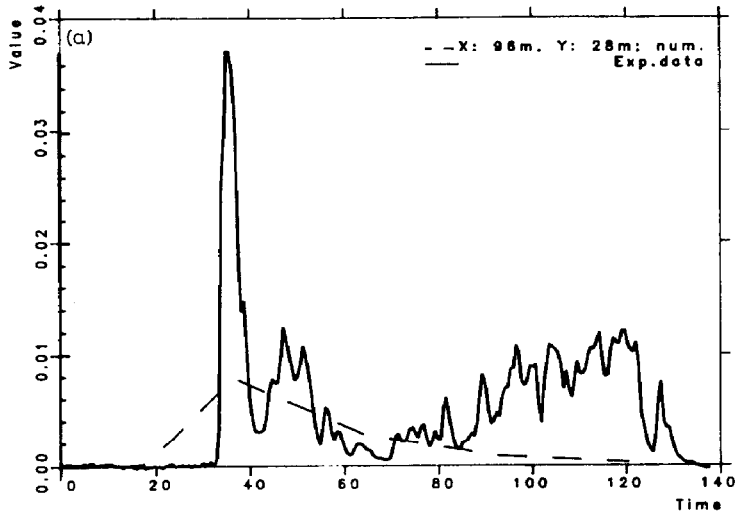

Fig. 9a. Concentration as a function of time at the height of 2.4 m. Numerical simulation compared with experimental data. Location coordinates (400,300).

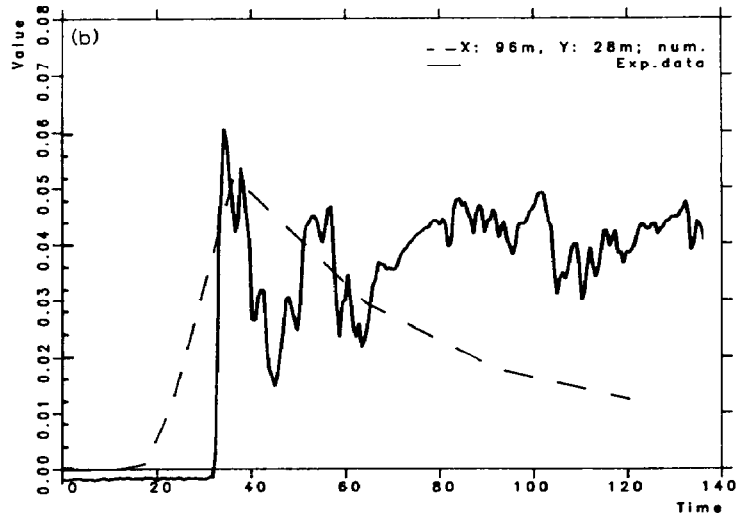

Fig. 9b. Concentration as a function of time at the height of 0.4 m. Numerical simulation compared with experimental data. Location coordinates (400,300).

vertical direction equal to 0.5 m. The smallest grid dimensions in the horizontal plane is 11.5 m in the downwind direction and half this value in the cross wind direction. The grid dimensions are too large to give a detailed description of the structure of the cloudfronts where the gradients are large, with respect to both the velocity and the concentration.

The tent containing the initial volume of gas in placed approximately 50 m

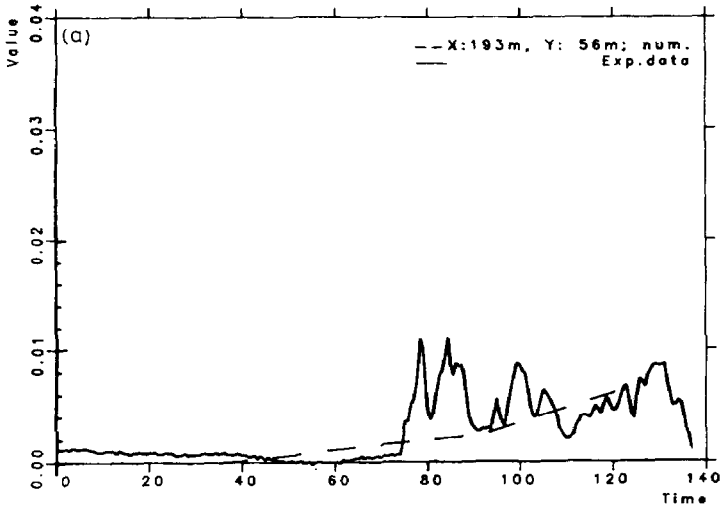

Fig. 10a. Concentration as a function of time at the height of 2.4 m. Numerical simulation compared with experimental data. Location coordinates (400,400).

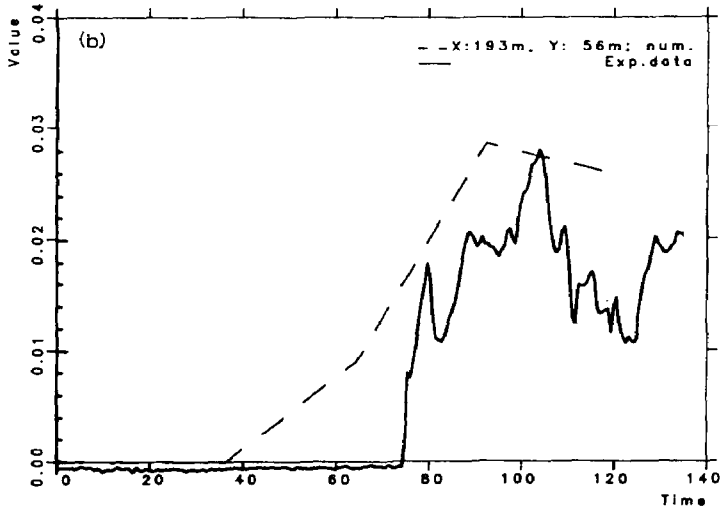

Fig. 10b. Concentration as a function of time at the height of 0.4 m. Numerical simulation compared with experimental data. Location coordinates (400,400).

from the upwind boundary and is assumed to be a rectangular box with sides equal to 11.50 m and height 13 m. The density of the ambient air was assumed to be 1.20 kg/m^3 while the density of the released gas was given as 2.06 kg/m^3.

4.2 Results and conclusions

With the given velocity profile as input value at the upwind boundary the velocity field was calculated before release.

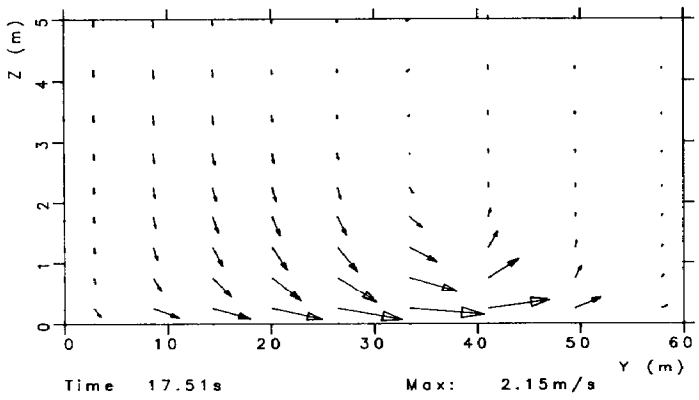

Fig. 11. Velocity components in a vertical crosswind plane 10 m behind the center of the initial gas column, $x = 10$, 17.5 s after release.

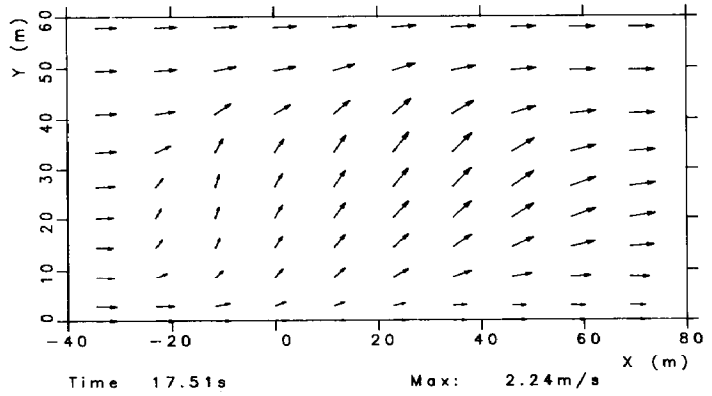

Fig. 12. Horizontal velocity components at the height of $z = 0.5$ m, 17. 5 s after release.

Figures 3 and 4 show the volume concentration in the cloud, at different times after the release, given in the vertical symmetry plane $y = 0$. Figures 5 and 6 show the same release viewed from above giving the volume concentration at the height of 0.4 m. Notice the differences in scale between Figs. 3 and 4 and between Figs. 5 and 6.

The calculations show that the dense part of the cloud is driven out from the center of the cloud where air is drawn down due to velocity field set up by the collapsing gas column. Some time after release we observe that the regions of the higher concentrations are found some distance away from symmetry line.

After 60 s the cloud has reached the boundary of the computational region and the calculations will probably give too high concentrations in the areas close to this boundary.

Figure 7 shows the coordinate system used in the calculations in relation to

the position of the measuring stations relevant for Trial 008. The results of the calculations are compared with the experimental data in Figs. 8–10.

Figure 11 shows the velocity components in a vertical plane normal to the mean wind direction at the position $x=10$. Near the cloud edge a vortex is found, but the resolution of the grid is too small to give a detailed picture of the front structure.

The horizontal velocity components are shown in Fig. 12 in the plane 0.5 m above the ground. At this height the cloud has a large influence on the local velocity field, but as Fig. 11 shows, at the height of 3 m the effect is rather small indicating a thin cloud down on the ground.

The resolution of the grid system is too small to predict the shorter transients shown by the data. The mean concentrations and the arrival of the cloud is, however, fairly well predicted especially for the lower parts of the cloud. Higher up above the ground the predictions are not so good.

This may be due to the fact that the mixing process is described by very simple relations and, thus only some parts of the cloud can be properly modelled. The upper part of the cloud is also more sensitive to changes in the windfield, and this effect is not included in the model which assumes a constant input velocity profile.

The computer program has here been applied to a transient release on a flat terrain without obstructions. It is, however, possible to include buildings and fences in the flowfield and thereby simulate the releases of Thorney Island trials Phase II.

Acknowledgement

This work was sponsored by Norsk Hydro A/S, Statoil A/S, Borregaard Ind. Ltd. and the Royal Norwegian Council for Scientific and Industrial Research.

List of symbols

c concentration (mass fraction)
c_{vol} volume concentration
g acceleration of gravity
k turbulent kinetic energy
p pressure
P production term
Pr Prandtl/Schmidt number
R specific gas constant
Ri Richardson number
S source term

t time
u horizontal velocity component in x-direction
v horizontal velocity component in y-direction
w vertical velocity component
x horizontal coordinate in the main wind direction
y horizontal coordinate normal to the x-direction
z vertical coordinate

Γ diffusion coefficient
ϵ dissipation
ρ density
τ shear stress
ϕ general variable

References

1 S.V. Patankar and D.B. Spalding, A calculation procedure for heat, mass and momentum transfer in three-dimensional parabolic flows. Int. J. Heat Mass Transfer, 15 (1972) 1787–1806.
2 D.M. Deaves, Application of advanced turbulence models in determining the structure and dispersion of heavy gas clouds, In: G. Ooms and H. Tennekes (Eds.), Proc. IUTAM Symposium, Delft, The Netherlands, 1983, Springer Verlag, 1984.
3 D.M. Deaves, Application of a turbulence flow model to heavy gas dispersion in complex situations, In: S. Hartwig (Ed.), Proc. 2nd Battelle Symposium on Heavy Gas and Risk Assessment, Frankfurt, 1982, D. Reidel, Dordrecht, 1983.
4 G. Berge, Transiente beregninger av kompressibel strøyming basert på trykk-korreksjonsmetoden (Transient calculations of compressible flows based upon pressure correction methods), SINTEF Report STF15 F84079, December 1984.
5 Ø. Jacobsen and B.F. Magnussen, Numerisk simulering av 2-dimensjonal tung-gass spredning (Numerical simulation of a 2-dimensional dispersion of heavy gas), SINTEF Report STF15 F86003, February 1986.
6 Y. Riou, Comparison between MERCURE-GL code calculations, wind tunnel measurements and Thorney Island field trials, J. Hazardous Materials, 16 (1987) 247–265.
7 W. Rodi, Turbulence models and their application in hydraulics – a state of the art review, IAHR Publ. 1980.